Pergamon

Int. J. Heat Mass Transfer. Vol. 37, No. 5, pp. 882–884, 1994

0017–9310/94 $6.00 + 0.00

The effect of grid size in near-wall k–ε calculations of mass transfer rates at high Schmidt numbers

J. HERRERO, F. X. GRAU, J. GRIFOLL and FRANCESC GIRALT
Escola Tècnica Superior d'Enginyeria, Universitat Rovira i Virgili, Tarragona, Catalunya, Spain

(*Received* 3 *August* 1993)

INTRODUCTION

THE USE of near-wall turbulence models is necessary for mass transfer computations at low diffusivity conditions. Few of the existent near-wall k–ε proposals yield, under the assumption of a constant turbulent Schmidt number, satisfactory predictions for mass transfer rates at high Schmidt numbers. In order to remedy this situation, Herrero *et al.* [1] developed a new k–ε formulation (H91) based on Lam and Bremhorst's model [2] (LB).

Nesic *et al.* [3] very recently simulated mass transfer rates in a sudden pipe expansion using the LB proposal. Although the Schmidt number studied was high enough ($Sc = 1460$), they did not choose a near-wall formulation suitable for low diffusivity conditions, such as H91 or Myong *et al.* [4]. Nesic *et al.* [3] concluded LB overpredicts experimental mass transfer rates with a $Sc_t = 0.9$, in both the recirculating and in the fully developed pipe flow regions. In order to force agreement with the experimental values of Berger and Hau [5] they propose $Sc_t = 1.7$ in the viscous sublayer ($y^+ < 5$) and $Sc_t = 0.9$ for $y^+ > 5$. H91 results, however, show that the LB formulation predicts Sherwood numbers in fully developed pipe flow that are half the value of Berger and Hau's experimental data. In order to clarify matters, a numerical simulation of momentum and mass transfer in a sudden pipe expansion is performed. Predictions are compared with the data reported by Sydberger and Lotz [6] at $Re = 42\,000$ and $Sc = 1460$, which were also used by Nesic *et al.* [3], and with those measured at $Sc = 2500$ by Runchal [7].

NUMERICAL PROCEDURE

The averaged governing equations with the original LB and the modified H91 damping functions, with $Sc_t = 0.9$, were solved for the primitive variables using staggered grids and a second order accurate procedure. A sufficient number of computational grid points, e.g. 4–5 mesh points, have to be adequately distributed within the viscous sublayer ($y^+ < 5$) when momentum transfer is computed. Mass transfer calculations require, in addition, that at least one computational point has to be placed in the linear concentration profiles region, i.e. for $Sc = 2500$ at least one point should be located at $y^+ = 0.1$, as used by Nesic *et al.* [3]. Care was also taken to have enough grid cells in regions of sudden pipe expansion where important velocity and concentration gradients occur.

The four different meshes described in Table 1 were used in the computations. Grids A and B consisted of 81 points in the axial direction and 28 points in the radial direction, so that the grid used by Nesic *et al.* [3] could be approximately reproduced. The distance between points in the radial direction is allowed to grow faster in grid A than in grid B. The finer grid C consists of 123×75 nodes. Although this mesh is sufficient for engineering calculations, an even finer grid of 188×127 nodes (grid D) was used to check that computations were grid independent. In all calculations the inlet/outlet diameter ratio was taken equal to 0.5. Grids A and B expand 10 outlet diameters in the direction of the flow, to reproduce Nesic *et al.*'s [3] conditions as closely as possible, while meshes C and D cover a total length of 80 diameters to observe the development of pipe flow.

The zero gradient boundary condition for the dissipation rate at the wall used by Nesic *et al.* [3] was also adopted in the present work, despite the fact that direct numerical simulation results indicate that this boundary condition is inadequate (Chapman and Kuhn [8]). However, no significant differences in the numerical results were observed when either the zero gradient or other alternative boundary conditions for ε, such as those proposed by Chapman and Kuhn [8] or Lam and Bremhorst [2], were applied. The turbulent kinetic energy of the inlet flow has a strong influence on the shape and characteristics of the recirculation, as discussed by So [9]. Since Sydberger and Lotz [6] and Runchal [7] do not report accurate values for the inlet conditions or for the reattachment length x_L, which in both cases it was comprised between 5.0 and 7.0 step heights h, the turbulence intensity value of 0.1 suggested by So [9] was used.

RESULTS AND DISCUSSION

Stanton numbers computed with the finest grids are compared in Figs. 1 and 2 with experimental data. Both LB and H91 models predict that maximum transfer rates occur close to the reattachment point, but values are clearly over-

Table 1. Summary of different computational grids used in present work

	Grid A	Grid B	Grid C	Grid D
Points in x direction	81	81	123	188
Points in y direction	28	28	75	127
First y distance (y^+)	0.1	0.1	0.1	0.1
First x distance (x/h)	0.02	0.02	0.02	0.002
Total pipe length (x/h)	38	38	320	320

NOMENCLATURE

h step height [m]
k turbulent kinetic energy [$m^2 s^{-2}$]
Re Reynolds number based on average velocity and diameter
Sc Schmidt number
Sc_t turbulent Schmidt number
St Stanton number
u_* friction velocity [$m s^{-1}$]
x axial coordinate [m]
x_L reattachment length [m]
y distance to pipe wall [m]
y^+ dimensionless distance to the wall, yu_*/ν.

Greek symbols
ε dissipation rate of k [$m^2 s^{-3}$]
ν kinematic viscosity [$m^2 s^{-1}$].

predicted. According to Launder [10], such behaviour is typical of low Reynolds number k–ε models, which tend to overpredict this maxima by a factor as large as seven. Both figures illustrate that the LB model yields a fully developed Stanton value much lower than that predicted by H91, which is in good agreement with experimental data.

The main trends observed in Figs. 1 and 2 are quantified in Table 2, where the fully developed values given by the correlation of Berger and Hau [5] are also included. For the case of $Sc = 1460$, the maximum peak values predicted by the LB and H91 formulations are 3.3 and 4.9 times larger than the experimental values reported by Sydberger and Lotz [6] near the reattachment point. The LB formulation, however, underpredicts the experimental fully developed values at $Sc = 1460$ and 2500 by 50%, whereas H91 is in reasonable agreement with data and the correlation of Berger and Hau [5]. It should be noted that when transfer rates are normalized with respect to fully developed pipe values LB predicts a ratio of 15.1 for the reattachment region, which is much larger than the 11.9 given by H91 or the experimental ratio of 2.4.

These results are in agreement with those reported by Herrero *et al.* [1]. However, they contradict the conclusion reached by Nesic *et al.* [3] that the LB formulation tends to overpredict the fully developed experimental values obtained from the correlation of Berger and Hau [5]. A possible explanation for this discrepancy is the fact that Nesic *et al.* [3] used in their work a coarse mesh, similar to present grid A. In order to establish the effects of grid size in the computations the four meshes A–D included in Table 1 have been used to predict mass transfer rates at $Sc = 1460$. Computed transfer rates are presented in Figs. 3 and 4 for both LB and H91 formulations. Figure 3 shows that predictions obtained with grid A, which has the last computational point in the streamwise direction placed at $x/h = 38$, differ significantly from those obtained using the other finer grids. Grid A yields higher Stanton numbers in the redeveloping region for both models. The same behaviour is observed in Fig. 4 for grid B. In this case, however, predictions are more similar to those of grids C and D because a more adequate grid distribution is applied.

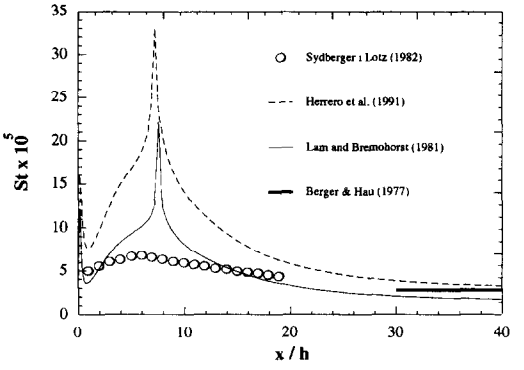

FIG. 1. Axial evolution of mass transfer rate at $Sc = 1460$.

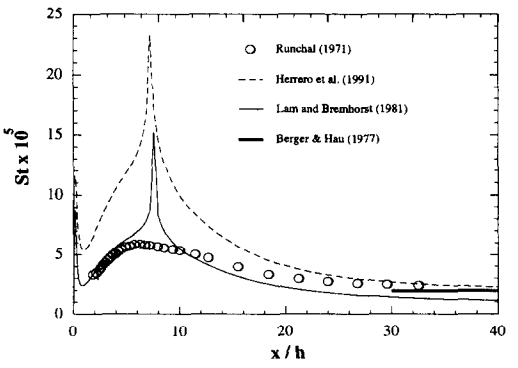

FIG. 2. Axial evolution of mass transfer rate at $Sc = 2500$.

Table 2. Comparison of predicted and experimental Stanton values at the maximum mass transfer location and in the fully developed region

	$Sc = 1460$		$Sc = 2500$	
$St \times 10^5$	Peak value	Fully dev. value	Peak value	Fully dev. value
LB	22.25	1.47	15.24	0.98
H91	33.1	2.79	23.3	1.94
Experiment	6.8	2.89	5.9	2.02

Table 3. Effect of computational grid on predicted mass transfer rates

	LB		H91	
$St \times 10^5$	Peak value	Value at $x_L/h = 38$	Peak value	Value at $x_L/h = 38$
Grid A	16.36	2.13	29.26	3.61
Grid B	15.76	1.77	29.44	3.11
Grid C	17.59	1.82	32.3	3.39
Grid D	22.25	1.79	33.1	3.36

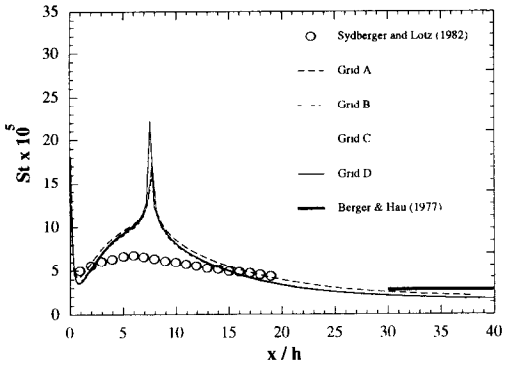

FIG. 3. Effect of computational grid on numerical predictions obtained with the LB formulation.

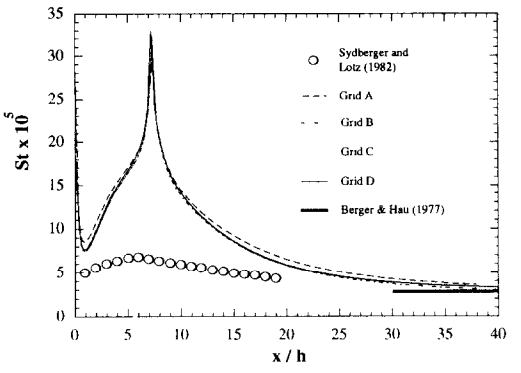

FIG. 4. Effect of computational grid on numerical predictions obtained with the H91 formulation.

Further comparison of grid performance is presented in Table 3. This table includes the values of the Stanton number at the location of maximum transfer rates and at $x/h = 38$. Mass transfer rates at $x/h = 38$ in Table 3 deviate more than 20% from the fully developed values included in Table 2. This indicates that the flow is not completely developed at that location. Furthermore, Table 3 shows that the coarser grids A and B yield Stanton values that differ clearly from those computed with grids C and D at both locations. The small discrepancies that are observed for the finest grids C and D, and which persist at $x/h = 320$, suggest that grid independence of results are only ensured for grid D in both the redeveloping and fully developed regions. The difference observed in the peak value for the LB simulation indicates that grid C is not fine enough in the region of separated flow.

Nesic *et al.* [3] report a computed value for the mass transfer rate at the peak location, obtained using the LB formulation, that is more than 20% lower than the lowest value shown in Table 3. In addition, their predictions at $x/h = 30$ are 100% higher than the highest values reported in this table. Thus, present results illustrate the importance of choosing appropriate grids for computation of mass and/or heat transfer rates, especially under low diffusivity conditions.

CONCLUSIONS

The numerical simulation of transfer rates in a sudden pipe expansion at $Re = 42\,000$ for $Sc = 1460$ and 2500 shows that few low Reynolds number k–ε formulations are capable of yielding accurate predictions under low diffusivity conditions. The performance of previous models is significantly affected by the size and node distribution of the computational grid used. Results show that coarse grids can yield predictions that are in error even in the fully developed pipe flow region. Under some circumstances these grids may even force models that otherwise perform poorly from a mass and/or heat transfer point of view to yield predictions in agreement with published data.

Acknowledgements—This work was financially supported by the CICYT, project PB88-0218. Computer support was granted by the Servei de Tecnologia Química, Universitat Rovira i Virgili, Tarragona.

REFERENCES

1. J. Herrero, F. X. Grau, J. Grifoll and F. Giralt, A near wall k–ε formulation for high Prandtl number heat transfer, *Int. J. Heat Mass Transfer* **34,** 711–721 (1991).
2. C. K. G. Lam and K. Bremhorst, A modified form of the k–ε model for predicting wall turbulence, *J. Fluids Engng* **103,** 456–460 (1981).
3. S. Nesic, J. Postlethwaite and D. J. Bergstrom, Calculation of wall-mass transfer rates in separated aqueous flow using a low Reynolds number k–ε model, *Int. J. Heat Mass Transfer* **35,** 1977–1985 (1992).
4. H. K. Myong, N. Kasagi and M. Hirata, Numerical prediction of turbulent pipe flow heat transfer for various Prandtl number fluids with the improved k–ε turbulence model, *JSME Int. J. II* **32,** 613–622 (1989).
5. F. P. Berger and K.-F. F.-L. Hau, Mass transfer in turbulent pipe flow measured by the electrochemical method, *Int. J. Heat Mass Transfer* **20,** 1185–1194 (1977).
6. T. Sydberger and U. Lotz, Relation between mass transfer and corrosion in a turbulent pipe flow, *J. Electrochem. Soc.* **129,** 276–283 (1982).
7. A. K. Runchal, Mass transfer investigation in turbulent flow downstream of sudden enlargement of a circular pipe for very high Schmidt numbers, *Int. J. Heat Mass Transfer* **14,** 781–792 (1971).
8. D. R. Chapman and G. Kuhn, The limiting behaviour of turbulence near a wall, *J. Fluid Mech.* **170,** 265–292 (1986).
9. R. M. C. So, Inlet centerline turbulence effects on reattachment length in axisymmetric sudden-expansion flows, *Exper. Fluids* **5,** 424–426 (1987).
10. B. E. Launder, On the computation of convective heat transfer in complex turbulent flows, *J. Fluid Engng ASME Trans.* **110,** 1112–1128 (1988).